

Coulomb blockade without potential barriers

Gabriel Vasseur, Dietmar Weinmann^a, and Rodolfo A. Jalabert

Institut de Physique et Chimie des Matériaux de Strasbourg,^b 23 rue du Loess, BP 43, 67034 Strasbourg cedex 2, France

28th June 2018

Abstract We study transport through a strongly correlated quantum dot and show that Coulomb blockade can appear even in the presence of perfect contacts. This conclusion arises from numerical calculations of the conductance for a microscopic model of spinless fermions in an interacting chain connected to each lead via a completely open channel. The dependence of the conductance on the gate voltage shows well defined Coulomb blockade peaks which are sharpened as the interaction strength is increased. Our numerics is based on the embedding method and the DMRG algorithm. We explain the emergence of Coulomb blockade with perfect contacts by a reduction of the effective coupling matrix elements between many-body states corresponding to successive particle numbers in the interacting region. A perturbative approach, valid in the strong interaction limit, yields an analytic expression for the interaction-induced suppression of the conductance in the Coulomb blockade regime.

PACS. 73.23.Hk Coulomb blockade; single-electron tunneling – 73.23.-b Electronic transport in mesoscopic systems – 71.27.+a Strongly correlated electron systems; heavy fermions

1 Introduction

The discreteness of the electron charge blocks the transport through a small and relatively isolated conductor (usually referred as a quantum dot) at sufficiently low temperature and bias voltage. This peculiar phenomenon, known as Coulomb blockade, is a paradigm in the physics of small condensed matter systems. The Coulomb blockade can be lifted by tuning a gate voltage to a point of degeneracy, where the energy cost for adding or removing an electron to the system vanishes. The obvious signature of large conductance oscillations as a function of gate voltage makes this phenomenon promising for applications, and at the same time a privileged set-up to investigate interactions in confined systems [1,2].

A question that has been present since the beginning of the studies on Coulomb blockade is: what are the minimum ingredients for it to be observed? The repulsive interparticle interaction is clearly one of them, as well as the condition that the charging energy of the dot be greater than the thermal energy $k_B T$ or the applied bias eV . Having an almost isolated dot, connected to conducting leads by weakly transmitting contacts like tunnel-barriers, has been thought to be another essential ingredient. Various studies have been undertaken to follow the evolution of the Coulomb blockade oscillations as the dot becomes better coupled to the leads.

It was in the quantum Hall regime that Coulomb blockade effects in open (well coupled) dots were initially

investigated [3,4]. The existence of spatially separated edge channels made it possible to observe conductance oscillations even in the case in which the point contacts at the entrance of the dot had a conductance G_B larger than the quantum conductance $G_0 = e^2/h$.

In the absence of the quantum Hall effect, the regime of weak Coulomb blockade, which is intermediate between that of strong Coulomb blockade ($G_B \ll G_0$) and the one of a large number of fully open channels ($G_B \gg G_0$, where no Coulomb blockade can be observed), has been studied [5,6]. In the regime of weak Coulomb blockade ($G_B \sim G_0$), the precise behaviour of the system depends on the way in which the value of the entrance conductance is obtained. In the case of metallic islands coupled to leads via tunnel-barriers, G_B can be of the order of G_0 due to a large number of weakly transmitting channels; while in semi-conducting dots coupled to leads via point contacts, conductances G_B of the order of G_0 are obtained by increasing the transmission of only a few channels.

Nazarov has shown that charge quantization may persist when the dot is connected to the leads via arbitrary conductors [7], as for example disordered metallic wires, instead of tunnel-barriers. In the general case of a number of not perfectly transmitting channels, the effective charging energy is exponentially small (scaling as $\exp(-G_B/G_0)$). However, the charging energy vanishes if one of the channels is perfectly transmitting.

It is important to make the distinction between perfect transmission and perfect contact. The notion of transmission of the barrier, which should be “measured” between two electrodes, may not be a relevant concept when the

^a *e-mail*: Dietmar.Weinmann@ipcms.u-strasbg.fr

^b UMR 7504 ULP-CNRS

barrier is between a dot and an electrode. In this case a perfect contact does not guarantee the absence of reflection, since electrons can be coherently backscattered inside the dot.

Recent works [8,6] considering open dots have taken into account the coherent backscattering induced by the dot itself. They found that interactions do not modify the average conductance when all the channels are either open or closed (case of ideal contacts). This conclusion is in agreement with an experiment performed on rather large chaotic dots [9].

Experimentally, Coulomb blockade physics has been observed recently in very small silicon based MOSFETs where the tunnel-barriers are not built-in [10,11]. It is likely that the Coulomb blockade features of these samples are due either to diffusive leads or to electrostatic potential barriers created between the dot and the leads. It is, however, of interest to study whether it is really necessary to have poor contacts for obtaining the Coulomb blockade. For dots of reduced dimensionality and containing a low number of electrons, we expect electronic correlations to be of crucial importance. Therefore we may ask whether Coulomb blockade can arise even with perfect contacts, due only to strong correlations.

In order to address this question, it is important to go beyond the usual treatment of the interactions in the dot based on the capacitive charging energy. Microscopic models of correlated chains attached to semi-infinite leads have recently been investigated [12,13,14]. For good but not perfect contacts, it has been found that Coulomb blockade-like features are reinforced by the interactions.

In this paper, we present a study of a microscopic model for a strongly correlated quantum dot and show that Coulomb blockade arises even in the presence of perfect contacts.

The model and the method are introduced in section 2. The numerical results presented in section 3 show that Coulomb blockade appears as the interaction strength increases, even in the absence of potential barriers between the dot and the leads. The features of the peaks and valleys are analyzed in detail in section 4 using perturbative approaches at weak transmission. In the concluding section, we discuss the implications of our findings and possible extensions of our model in order to approach the current experimental setups.

2 Embedding method for the conductance of a one-dimensional model

Most of the analytical approaches to Coulomb blockade rely on the so-called constant charging model, where correlations are completely disregarded. The only electron-electron interaction term considered is the capacitive charging energy of the quantum dot. While various refinements, such as the Random Phase Approximation [15], have been developed to describe the case of small dots with poor screening, treating electronic correlations to all orders is obviously out of reach in any analytical approach.

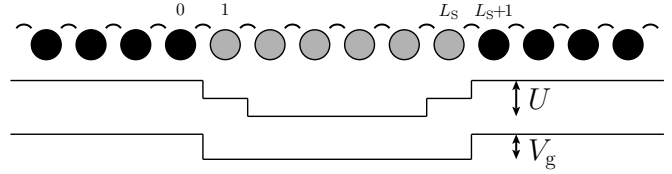


Figure 1. The central region of an infinitely long, one-dimensional chain. The particles experience nearest neighbour interaction of strength U on sites 1 to L_S . Below the chain are sketched the compensating potential of the interaction (see text) and the potential due to the gate voltage V_g .

Numerically, various schemes for obtaining the addition spectrum of a quantum dot have been used [16]. However, these calculations of ground state energies cannot capture the richness and complexity of a transport problem, especially for open quantum dots.

Even numerically, the transport through strongly correlated systems has remained an intractable problem until recently. The development of the so-called embedding method [17,18] has been an important advance in this difficult problem. Relating the transport properties of a quantum dot with the thermodynamic properties of the combined system (sample + leads, as we explain in the sequel), allows to extract the conductance through the dot from the numerically accessible ground state energy of the combined system.

The embedding method can readily be used for spinless fermions (spin-polarized electrons) in one-dimensional chains. While the method has been successfully generalized to spin-half electrons [19], the problem of spinless fermions remains more easily tractable. For these reasons we restrict ourselves in this work to one-dimensional spinless fermions. It is expected that the qualitative aspects of our results apply also in higher dimensions and once we take the electron spin into account.

We consider a model of spinless fermions in a chain, as sketched in Fig. 1. The dot corresponds to a region of length L_S in which the particles are interacting. In the rest of the chain, representing the leads of the standard experimental set-up, the particles do not interact. Therefore, far away from the dot, a Fermi energy E_F is well-defined. We fix the latter to the centre of the band, corresponding to half filling. The Hamiltonian of the whole system reads

$$H = H_K + H_U + H_G, \quad (1)$$

where

$$H_K = - \sum_{i=-\infty}^{\infty} (c_i^\dagger c_{i+1} + h.c.) \quad (2)$$

stands for the kinetic energy of an ideal one-dimensional chain. Here, c_i annihilates a particle on site i . Setting the hopping amplitudes in H_K to unity defines our energy scale.

The dot is represented by the sites $i = 1$ to L_S (the lattice constant is set to unity). The inter-particle interaction

$$H_U = U \sum_{i=1}^{L_S-1} (\hat{n}_i - 1/2)(\hat{n}_{i+1} - 1/2) \quad (3)$$

acts only in this region and is assumed to be restricted to nearest neighbours (with strength U and $\hat{n}_i = c_i^\dagger c_i$). H_U includes a one-body compensating potential (due to the presence of the $1/2$'s, see Fig. 1) which ensures, in the absence of gate voltage, particle-hole symmetry even at $U \neq 0$. It can be seen as a positive background that prevents the particles from leaking out of the dot region, in spite of the interaction. Additional particles can then be attracted in the dot by the one-body potential

$$H_G = -V_g \sum_{i=1}^{L_S} \hat{n}_i \quad (4)$$

describing the effect of an applied gate voltage V_g .

The relative isolation of a dot is usually achieved by connecting it to the leads via weak links or tunnel-barriers (*i.e.* by choosing a smaller hopping amplitude or a high on-site potential), but we do not take any of these approaches in this work. In contrast, in our case, *the contacts between the dot and the leads are perfect*. The dot is therefore only defined by the region where the electron-electron interactions and the gate voltage are present.

We use the embedding method which allows to determine the modulus $|t|$ of the effective transmission amplitude $t = |t|e^{i\alpha}$ of the system at the Fermi energy of the electrodes, taking fully into account the effects of electronic correlations. This thereby yields the zero-temperature, linear-response conductance $g = |t|^2$ (in units of e^2/h). The modulus $|t|$ is obtained from the persistent current flowing in a ring formed by the interacting dot together with an infinitely long, non-interacting lead.

The relation between the persistent current and the conductance is based on two facts, which are both realized in the limit of an infinitely long lead. First, the persistent current in a ring including a *one-body* (non-interacting) scatterer only depends, in this limit, on the modulus $|t|$ of the transmission amplitude of the scatterer. Second, it is only in the limit of an infinitely long lead that a ring containing an *interacting part* behaves as a Fermi liquid, and that a one-body transmission amplitude t can be attributed to the interacting region attached to leads [20].

The study of closed, finite-size systems thus allows to obtain the Landauer conductance of the dot in the setup described by the Hamiltonian (1), provided that an extrapolation to infinite size is performed. We are able to perform reliable extrapolations for an interacting dot of $L_S = 6$, even near the resonances, where the extrapolation procedure is most difficult [18]. Therefore, besides the results for the physics of Coulomb blockade, this work also constitutes a test of the embedding method in a computationally demanding situation.

To be specific, we use the phase sensitivity $\mathcal{D} = (L/2)|E_P - E_A|$, where $E_{P,A}$ denotes the ground state energies of the ring for periodic (antiperiodic) boundary conditions, and L is the total size of the ring. The extrapolation to $L \rightarrow \infty$ is carried out from data calculated for different ring sizes. The limiting value \mathcal{D}_∞ leads to the effective transmission amplitude of the system at the Fermi energy [17,21]

$$|t| = \sin(\mathcal{D}_\infty). \quad (5)$$

Similar approaches using the persistent current have also been recently proposed [22,23,24].

We take advantage of the efficiency of the Density Matrix Renormalization Group algorithm (DMRG) [25,26] which allows to calculate \mathcal{D} with very high precision, taking fully into account the electronic correlations. The extrapolation can then usually be performed from the many-body ground state energies of rings of up to 100 sites. Near the resonances, however, the extrapolation can be quite difficult and we need to treat rings containing up to 300 sites, keeping up to 1000 states in the DMRG iterations.

3 Interaction-induced conductance oscillations as a function of gate voltage

The dimensionless conductance g as a function of the gate voltage V_g is shown in Fig. 2, together with the mean charge inside the dot region. The three graphs shown are for a dot of length $L_S = 6$, and different interaction strengths.

The non-interacting case ($U = 0$, Fig. 2a) corresponds to free particles in a chain with a potential well of length L_S and depth V_g . The structures in the conductance for this case can be understood from one-body quantum transport through the well potential, and thus $t(E_F) = |t|e^{i\alpha}$ can be readily calculated. The conductance is then obtained as $g = |t|^2$ which, when $|V_g| \leq 2$ and for $E_F = 0$, can be written as

$$|t|^2 = \left(\cos^2(f(V_g)L_S) + \frac{\sin^2(f(V_g)L_S)}{\sin^2(f(V_g))} \right)^{-1}, \quad (6)$$

with $f(V_g) = \arccos(-V_g/2)$. The result, plotted in Fig. 2a, is in perfect agreement with the numerical data obtained from the embedding method. This is a stringent test of our method since the non-interacting case does not represent a special situation for the DMRG algorithm. Furthermore, the transmission phase α can be related to the number N of particles inside the dot by the Friedel sum rule [27,28]

$$N_d = \alpha/\pi, \quad (7)$$

where N_d is the number of particles displaced by the dot. N_d gives the number N of particles *inside* the dot only for a system with homogeneous density, such that deviations between the analytic result (dotted line in Fig. 2a) and the DMRG data appear with increasing gate voltage, when part of the displaced particles are in the leads. We also calculated N from a direct diagonalization of the one-body Hamiltonian, and find perfect agreement with the DMRG data (see Fig. 2a, dashed line).

As one increases the interaction, a *well-defined peak structure appears*. The electron-electron interaction suppresses the conductance between the peaks which become sharper with increasing interaction strength. This tendency can be observed already at moderate interaction strength $U = 2$ (Fig. 2b), and becomes very pronounced at strong interaction $U = 10$, as can be seen in Fig. 2c. In

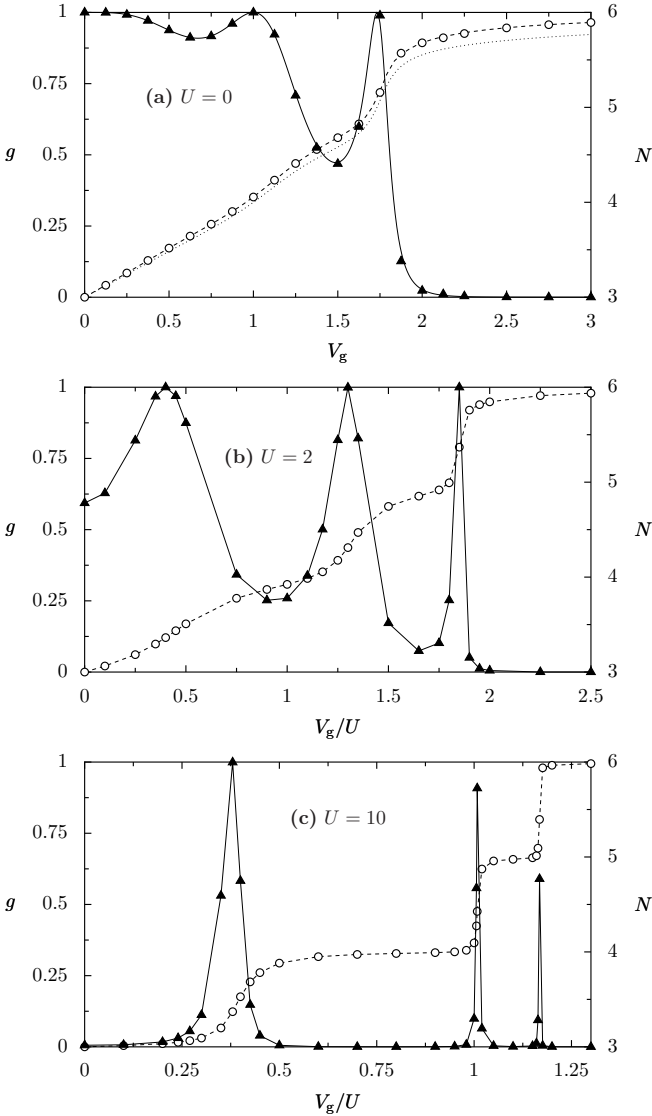


Figure 2. Dimensionless conductance g (triangles) and mean number of particles N (circles) inside the dot (of $L_S = 6$ sites), as a function of the gate voltage V_g without interaction **(a)** and V_g/U for $U = 2$ **(b)** and $U = 10$ **(c)**, obtained by DMRG calculations. In the non-interacting case **(a)**, g is known analytically (Eq. (6), solid line). The Friedel sum rule (dotted line) gives N approximately (see text) while one-body numerics (dashed line) is in perfect agreement with the DMRG points. In **(b)** and **(c)** lines are guides to the eye.

a one-body problem with symmetric contacts the conductance at resonance reaches unity. In our strongly correlated problem the limited amount of data points and the uncertainty of the extrapolation do not allow to settle the precise values at resonance in Fig. 2c.

The emergence of a well-defined peak structure in the conductance g is accompanied by the appearance of a staircase dependence on V_g of the mean particle number N inside the dot region. *The plateaus appear at integer values of the mean particle number*, and the steps in N

occur precisely at the gate voltage values of the conductance peaks.

Although the dot region is perfectly connected to the leads, these structures are clearly due to the Coulomb blockade effect, and their features can be identified with the properties of the usual Coulomb blockade conductance oscillations. It therefore appears that the dot becomes effectively decoupled from the leads by the electron-electron interaction. The underlying mechanism will be discussed in the following sections. In particular, we will show in section 4.2 that when the interaction is strong enough, the peak positions can be predicted precisely from the knowledge of the ground state energies of the isolated dot system for different mean particle numbers. Similar conclusions have been drawn from numerical studies of a chain containing 7 sites, but connected to the leads by reduced hopping matrix elements [13,14]. In this case, a DMRG evaluation of the Kubo formula and a DMRG study of the real-time dynamics have been performed showing a reinforcement of Coulomb blockade features when the interaction strength is increased. Including the spin degree of freedom leads to the appearance of conductance plateaus in the Kondo regime. A numerical renormalization group (NRG) study [12] of a Hubbard chain of 4 sites with moderate interaction strength and reduced coupling to the leads shows that the corresponding features are smoothed when the coupling to the leads is increased.

Since the full Hamiltonian is symmetric under the exchange of particles and holes with a simultaneous reversal of the sign of the gate voltage, the results for negative gate voltage can be obtained directly from the data presented in Fig. 2. The conductance is symmetric with respect to the gate voltage, $g(-V_g) = g(V_g)$, while the number of particles exhibits the property $N(-V_g) = L_S - N(V_g)$. Thus, as expected for a dot with $L_S = 6$ sites, there is a total of 6 peaks with the particle number increasing in steps from 0 to 6. Systems with larger L_S are therefore expected to give qualitatively similar results with L_S conductance peaks and L_S charge steps. In the case of odd L_S , the number of conductance peaks is odd. Because the conductance is an even function of the gate voltage, one of the conductance peaks must be at $V_g = 0$, in contrast to the case of even L_S , where $V_g = 0$ is always in the centre of a valley between two conductance peaks. This observation allows to understand the even-odd oscillations in the conductance of an interacting chain without gate voltage [17] discussed in detail in Ref. [29]. The oscillations of the conductance with the length of the interacting region are a very general feature of interacting chains. A perturbative treatment of the interactions [30] indicates that they appear in Hubbard chains as well. They may be related to experimentally observed conductance oscillations with the length of mono-atomic chains [31].

4 Perturbative approaches for weak transmission

In order to develop our understanding of the physical features found numerically, we present an analytical study of

the model for the regime of strong interaction. The behaviour observed in Fig. 2, and discussed in the previous section, indicates that the dot becomes decoupled from the leads when the interaction strength is increased. We will show that this is indeed the case. To this end, we treat the conductance through the system with a Fermi golden rule approach, valid when the effective coupling between the dot and the leads is small. In such a framework, the starting point is a dot region which is isolated from the leads. The coupling between the dot and the leads is then treated as a perturbation. In this case, the relevant coupling is not given by the one-body hopping amplitude between the sites $0 \leftrightarrow 1$ and $L_S \leftrightarrow L_S + 1$, which in our model is always unity, but by the matrix elements of the terms of the Hamiltonian (1) which couple the interacting dot region to the semi-infinite leads, sandwiched between the full many-body states of the chain. This coupling part of the Hamiltonian reads

$$H_C = -(c_0^\dagger c_1 + h.c.) - (c_{L_S}^\dagger c_{L_S+1} + h.c.) \quad (8)$$

and corresponds to H_K restricted to the two links between the dot and the leads. We now evaluate the lowest order contribution in H_C to the conductance of our system. In the case where the involved matrix elements of H_C are small (compared to U), the conductance is dominated by this term.

The conductance is related to the transmission of electrons through the system. Let us start by considering Fermi's golden rule for the transition rate

$$\gamma_{i \rightarrow f} = \frac{2\pi}{\hbar} |M_{f,i}|^2 \delta(E_f - E_i) \quad (9)$$

of a particle through the dot region. The initial state

$$|i\rangle = |k^{\text{left}}\rangle \otimes |0(N)\rangle \quad (10)$$

describes a product state built from eigenstates of the isolated dot and the semi-infinite leads. Here, we take the dot in its N -particle ground state $|0(N)\rangle$ and an additional particle $|k^{\text{left}}\rangle$ with wavenumber k in the left lead. In the final state

$$|f\rangle = |0(N)\rangle \otimes |k^{\text{right}}\rangle \quad (11)$$

the additional particle appears in the right lead while the dot returns to its N -particle ground state. The effective transition matrix element is of second order in H_C , and can be written as

$$M_{f,i} = \sum_{\alpha} \frac{\langle i|H_C|\alpha\rangle \langle \alpha|H_C|f\rangle}{E_i - E_{\alpha}}. \quad (12)$$

Here, the sum runs over all intermediate states $|\alpha\rangle$ corresponding to $N+1$ particles in the dot region and the Fermi vacuum in the leads or to $N-1$ particles in the dot and both leads occupied by an extra particle. Summing the transition rate (9) over the states of the non-interacting leads in a small energy interval corresponding to an infinitesimal bias voltage V , one can obtain the corresponding current and thus the dimensionless conductance

$$g = 4\pi^2 \rho^2 |M_{f,i}|^2, \quad (13)$$

where ρ is the density of states in the leads.

The approach is justified when the effective coupling given by the matrix element in Eq. (12) is small. This is the case at large U when the energy denominator is large, even though we have perfect contacts and H_C is not small. In addition, the matrix elements of H_C can be reduced due to the interaction-induced modification of the dot wavefunctions.

4.1 Conductance in the limit of strong interactions

In the strong interaction limit ($U \gg 1, V_g$), the ground state of the isolated dot region for an even dot length L_S at half filling ($N = L_S/2$) is given by a charge density wave (or Mott insulator, where the particles occupy alternating sites). In this case we can evaluate $M_{f,i}$, and hence obtain the conductance (13) in the corresponding conductance valley.

In this section, we treat not only the coupling between the dot and the leads, but also all of the hopping terms H_K as a perturbation to the other terms $H_0 = H_U + H_G$ of the Hamiltonian. This corresponds to an expansion in $1/U$ and follows the spirit of the large U expansions of the persistent current presented in Ref. [32]. In the absence of H_K , the two realizations of the Mott insulator with the particles on the even sites $|\psi_0^e\rangle = c_2^\dagger c_4^\dagger \dots c_{L_S}^\dagger |0\rangle$ and on the odd sites $|\psi_0^o\rangle = c_1^\dagger c_3^\dagger \dots c_{L_S-1}^\dagger |0\rangle$ are degenerate. They become coupled in N th order in H_K . The degeneracy is therefore lifted even for infinitesimal $1/U$ and the ground state is given by the symmetric (the effective coupling is $-(1/U)^{L_S/2}$) superposition

$$|\psi_0\rangle = \frac{1}{\sqrt{2}} (|\psi_0^e\rangle + |\psi_0^o\rangle). \quad (14)$$

In the leads, H_K yields plane wave eigenstates with the boundary condition that, due to the Mott-Hubbard gap (of the order of U), their wave-function vanishes (like $1/U$) on the first interacting site. For leads of length L on either side of the system this gives one-body states with energy $\epsilon_k = -2 \cos(k)$ and wave-functions $\langle i|k^{\text{left}}\rangle = \sqrt{2/L} \sin(k(1-i))$ on the left hand side ($i < 1$) and $\langle i|k^{\text{right}}\rangle = \sqrt{2/L} \sin(k(i-L_S))$ on the right hand side ($i > L_S$) of the interacting region.

Zero-temperature transport through the interacting segment of the chain requires that particles are transmitted elastically. Therefore, we need the lowest order processes in $1/U$ linking the initial state $|i\rangle = |k^{\text{left}}\rangle \otimes |\psi_0\rangle$ to the final state $|f\rangle = |\psi_0\rangle \otimes |k^{\text{right}}\rangle$. These processes are the ones in which a particle is transmitted while the component $|\psi_0^e\rangle$ of the ground state (14) of the interacting region is connected to the component $|\psi_0^o\rangle$ by sequences of $N+1$ successive single particle hoppings. In such a process, each of the N particles inside the interacting region hops to the next site, and hence the one initially sitting on site L_S leaves the region towards the right lead. In addition, a particle from the left lead enters the dot region and appears on site 1. An example of such a sequence is sketched in Fig. 3.

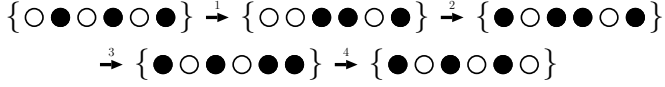


Figure 3. Example of a hopping sequence of $L_S/2 + 1 = 4$ hops connecting the two components of the ground state (14) of the uncoupled dot. Full and empty circles represent occupied and empty sites, respectively. In this example, a particle enters from the left in the second hop, and another one leaves it to the right in the last hop.

These dominating processes in the transport through an interacting chain are similar to the co-tunneling processes through arrays of quantum dots [5].

The lowest contributions to the effective matrix element $M_{f,i}$ are therefore of order $N + 1$ in H_K . It is given by

$$M_{f,i} = \sum_{S=\{\alpha_1, \alpha_2, \dots, \alpha_N\}} \frac{\langle i | H_K | \alpha_1 \rangle \langle \alpha_1 | H_K | \alpha_2 \rangle \dots \langle \alpha_N | H_K | f \rangle}{(E_i - E_{\alpha_1})(E_i - E_{\alpha_2}) \dots (E_i - E_{\alpha_N})}, \quad (15)$$

where $S = \{\alpha_1, \alpha_2, \dots, \alpha_N\}$ are sequences of N intermediate eigenstates of H_0 linked by $N + 1$ subsequent single particle hoppings. For all the $(N + 1)!$ different permutations of the order of the hops, the numerator is given by $(-1)^{N+1} \sin^2(k)/L$. The denominator involves U and V_g and depends on the sequence. For small even L_S we have explicitly derived the formula

$$M_{f,i} = -\frac{1}{L} \sin^2(k) \left(\frac{U}{V_g^2 - U^2/4} \right)^{L_S/2} \quad (16)$$

and we have confirmed its validity for larger values of L_S by performing the summation over the sequences numerically. With (13) and the one-dimensional density of states $\rho = L/(2\pi \sin(k))$ we get

$$g = \left(\frac{U}{V_g^2 - U^2/4} \right)^{L_S} \quad (17)$$

for the dominating contribution to the conductance in the limit of very strong interaction strength U , at $E_F = 0$ ($k_F = \pi/2$). This demonstrates that *Coulomb blockade eventually occurs for sufficiently strong interactions*. The suppression of the conductance in the valley due to the Mott insulating behaviour follows a power law in the interaction strength U and is exponential in the dot length L_S . The result of Eq. (17) is a generalization of the result found for $V_g = 0$ in [18]. The small values of the conductance around $V_g = 0$ in Fig. 2c are well described by Eq. (17) and the agreement improves for stronger interaction.

The power-law decay in Eq. (17) of the valley conductance with very large interaction strength U is obtained analytically and confirmed by very accurate numerics in our case of spinless fermions. For the case of Hubbard chains, an exponential decay was concluded [33] from NRG data for relatively moderate values of the interaction. However, our analytical approach can be applied to the Hubbard case as well, leading to a power law dependence of the conductance on the interaction strength

in the limit of large interaction strength. This power law is a consequence of the lattice model. The exponential decay mentioned in [33] might be an apparent dependence in a regime of intermediate interaction strength.

Within the same model, but in the absence of a gate voltage, it was previously found [17] that the smoothing of the contacts (i.e. the slow branching of the interaction going from the leads to the dot) reduces the interaction-induced suppression of the conductance found for even values of L_S . In the framework of the present paper, this means that smoothing the contacts will reduce the depth of the conductance valley at zero gate voltage. However, an adiabatic branching of the interaction is necessary to recover the perfect conductance found without interaction. Furthermore, numerical results [34] show that smoothing the interaction does not necessarily suppress the other valleys.

4.2 Peak positions and shapes

From the data presented on Fig. 2, the positions $V_g^{(N)}$ of the resonances can be determined as the gate voltage values for which there are precisely $N - 1/2$ particles inside the dot. These peak positions $V_g^{(N)}$, in units of U , are shown in Fig. 4 (symbols) as a function of the interaction strength U , together with the positions

$$\tilde{V}_g^{(N)}(U) = E_0(N, U) - E_0(N - 1, U), \quad (18)$$

that are obtained from the many-body energies $E_0(N, U)$ of the isolated dot with N particles (lines). One can see that already for $U = 10$, the positions of the resonances are very close to the isolated dot prediction of Eq. (18). This is an additional confirmation of the fact that the interaction leads to a decoupling of the dot from the leads.

One of the most relevant features of the numerical results shown in Fig. 2 is the sharpening of the conductance peaks with increasing interaction strength. We shall now provide an understanding for the effect of strong interactions on the peak width.

The width Γ_N of a peak is given by the value of the matrix element of H_C in the numerator of (12). Since the conductance resonance at $V_g^{(N)}$ is given by the degeneracy of the N - and $N - 1$ -particle ground states, we restrict our discussion to the contribution of the transition between those two ground states. Within a qualitative discussion, we can characterize the parameter dependence of the peak width using the transition matrix element

$$-\langle k_F^{\text{left}} | \otimes \langle 0(N - 1) | c_0^\dagger c_1 | 0(N) \rangle, \quad (19)$$

which contains the amplitude

$$\mathcal{E}_N = \langle 0(N - 1) | c_1 | 0(N) \rangle. \quad (20)$$

The main contribution to Γ_N is proportional to $|\mathcal{E}_N|^2$. This matrix element depends on the many-body wavefunctions, and is therefore strongly influenced by the interactions. For general values of N , it can be highly non-trivial to determine the ground state of the isolated dot.

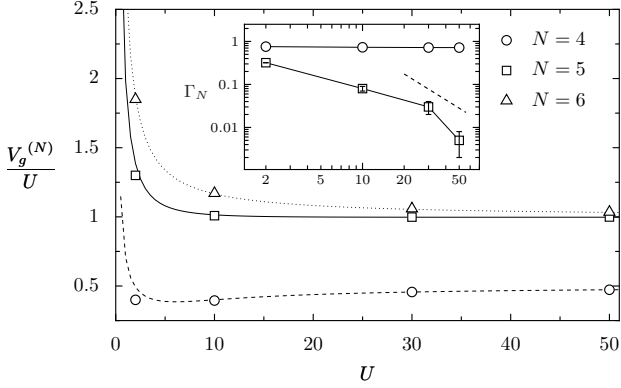


Figure 4. Positions $V_g^{(N)}/U$ of the peaks from the numerically obtained conductance (as in Fig. 2) as a function of the interaction strength U (symbols). The lines give the isolated dot prediction $\tilde{V}_g^{(N)}/U$ according to Eq. (18). The inset shows the peak width Γ_N as a function of U in double logarithmic scale. The error bars are given by the uncertainty of the fitting. For $N = 4$ they are smaller than the symbol size. The $N = 6$ data points (not shown) are the lowest and exhibit the largest error bars. The dashed line represents the asymptotic power law $1/U^2$.

There are, however, particular values of N for which we can study \mathcal{C}_N analytically.

One of these special values in the case of even L_S is $N = L_S/2 + 1$, which corresponds to the left peak in Fig. 2. In the limit of strong interactions, the $|0(N-1)\rangle$ state is a superposition of two charge density wave configurations, as presented in Eq. (14). The additional particle in $|0(N)\rangle$ is a defect (with interaction energy U) of the Mott insulator which can propagate freely, and can be described by an effective one-particle theory. In the absence of the kinetic energy H_K , the state $|0(N)\rangle$ is a superposition of the $L_S/2$ degenerate low-lying states of the form $c_1^\dagger c_3^\dagger \dots c_{2i-1}^\dagger c_{2i}^\dagger \dots c_{L_S}^\dagger |0\rangle$. In the presence of H_K , the weights of the different components are obtained by solving the equivalent problem of a free particle on $L_S/2$ sites. Only the weight of the first state (namely for $i = 1$) enters the expression for $\mathcal{C}_{L_S/2+1}$, and one obtains

$$\mathcal{C}_{L_S/2+1} = \frac{1}{\sqrt{L_S/2+1}} \sin\left(\frac{\pi}{L_S/2+1}\right). \quad (21)$$

In this limit of strong interaction, the lowest order contribution to $\mathcal{C}_{L_S/2+1}$ is thus independent of U (the limiting value is reached already for $U \gtrsim 2$ as can be seen in the inset of Fig. 4), but decreases as $L_S^{-3/2}$ with the length of the system when L_S is large, indicating a decrease of the peak width proportional to L_S^{-3} .

It is of some interest to compare this behaviour at large L_S with a non-interacting evaluation of the matrix element which one can calculate although at $U = 0$ the dot is not decoupled from the leads. In this non-interacting case, the eigenstates are given by free particles on L_S sites. $\mathcal{C}_{L_S/2+1}$ is then obtained from the value of the $(L_S/2+1)$ th lowest one-body wave-function on the first site. This leads to a size dependence of the matrix element as $L_S^{-1/2}$ only.

From this, one may conclude that the interactions play an important role in narrowing the resonance.

The other case in which analytical calculations are straightforward is the one of the last peak when $N = L_S$. In this case $|0(N)\rangle$ corresponds to the full dot. The state $|0(N-1)\rangle$ corresponds to one hole in a potential well with $U/2$ steps on the edges (as sketched in Fig. 1). It is obvious that when U increases, the hole is less likely to be found on an edge site, because of the potential step. The ground state of such a one-body system is solved by the ansatz of an even wave-function with $\psi(1 < n < L_S) = A \cos(k(n - (L_S + 1)/2))$ and $\psi(1) = \psi(L_S) = B$. The normalization allows to get B , which yields

$$\mathcal{C}_{L_S} = \frac{\cos\left(\frac{L_S-1}{2}k\right)}{\sqrt{\sum_{n=1}^{L_S} \cos^2\left(\left(n - \frac{L_S+1}{2}\right)k\right)}}, \quad (22)$$

where k is the smallest positive value that satisfies the condition

$$\cos\left(\frac{L_S+1}{2}k\right) = \frac{-U}{2} \cos\left(\frac{L_S-1}{2}k\right). \quad (23)$$

In this case, it can be seen that \mathcal{C} depends on U via k . In the limit of strong interaction, (23) can only be fulfilled if $\cos\left(\frac{L_S-1}{2}k\right) \sim U^{-1}$. This implies that the numerator of (22) decreases proportionally to U^{-1} and thus the peak width Γ_N is expected to decrease as U^{-2} . This impressive example of the reduction of the peak width due to the interaction is illustrated in the inset of the Fig. 4.

We end this section with a discussion on the symmetry of the peaks. As can be seen in Fig. 2c, the conductance peaks are not of symmetric Lorentzian shape. This is most obvious for the first peak and can be explained by an asymmetry in the coupling of the many-body states to higher and lower mean particle numbers. In order to understand this, we consider the representation of the matrix element $M_{f,i}$ as a single sum over the eigenstates $|\alpha\rangle$ of the isolated dot, as in Eq. (12).

Outside resonances, the number N of particles inside the dot, and therefore the initial (10) and final (11) states, are well-defined, and one can use Eq. (13) to evaluate the conductance. Very close to the conductance peak however, the transmission becomes large and the Fermi golden rule approach is not valid. To address the issue of the asymmetry of the peak, we consider values of the gate voltage which are in the vicinity of a resonance $V_g^{(N)}$ (and away from all the other), but far enough from the peak centre to have a small conductance. In this way, the conductance in the tails of the peaks can be treated using (12) and (13).

The main contributions to the sum (12) depend on whether the gate voltage is above or below the resonance value $V_g^{(N)}$. This resonance corresponds to the transition from $N-1$ to N particles in the dot.

For gate voltage values below the resonance, the states $|i\rangle$ and $|f\rangle$ are $N-1$ -particle states, and the most important contributions to $M_{f,i}$ come from the sum over the states $|\alpha\rangle$ with N particles inside the dot. The terms with $N-2$ particle states $|\alpha\rangle$ are suppressed by the much larger

energy denominator in (12). For gate voltages slightly above $V_g^{(N)}$, the initial and final states are N -particle states and the main contributions to the sum are due to intermediate $N - 1$ -particle states.

Since the many-body excitation spectrum of the isolated dot can depend dramatically on N , the sum can give very different results on the two sides of the peaks, which are therefore expected not to be symmetric.

We illustrate this mechanism for the example of the first peak of Fig. 2c, corresponding to the transition between half filling, $N - 1 = L_S/2 = 3$, and $N = 4$. On the left-hand side of this peak, the sum is dominated by the intermediate 4-particle eigenstates of the isolated dot, while the evaluation of the conductance on the right-hand side of the peak is dominated by the 3-particle eigenstates of the dot. The 3-particle spectrum of the dot is characterized by the Mott-gap which is of the order of U . The contribution of the excited 3-particle states is therefore suppressed by energy denominators of the order of U , leading to a smaller value of $M_{f,i}$ on the right-hand side of the peak than on the left-hand side, thus explaining the peak asymmetry observed on Fig. 2c.

5 Conclusion

We have shown that Coulomb blockade physics can occur when an interacting system is coupled to leads by perfect contacts. The underlying mechanism is that while the contacts are perfect on the one-particle level, the interaction can introduce many-body effects which effectively reduce the coupling between the interacting system and the leads.

In order to illustrate this peculiar behaviour, we have studied the gate-voltage dependence of the conductance through a one-dimensional chain in which spinless fermions are strongly interacting. We have used the embedding method to compute the conductance g and the mean number N of electrons inside the interacting chain from numerical DMRG data for the many-body ground state properties of large rings. This approach takes into account all the electronic correlations. Despite the absence of potential barriers separating the interacting chain from the leads, the numerical results in the regime of strong interaction unambiguously show features which are characteristic of Coulomb blockade physics in the transport through quantum dots. Peaks appear in the gate-voltage dependence of g , which are accompanied by steps in N . These structures become more and more pronounced, and the conductance becomes more and more suppressed in the valleys between the peaks, as the interaction strength is increased.

Our results indicate that, in spite of the perfect contacts, many-body effects lead to an effective decoupling of the interacting chain from the leads when the interaction is sufficiently strong. One can then consider the interacting part of the chain as a quantum dot. In order to interpret these results, we presented an analytical study of the model. We explained the deepening of the valleys (and therefore the occurrence of Coulomb blockade

itself) from a perturbative calculation of the conductance in the regime of strong interaction. In addition, we showed that the positions of the peaks can be deduced from the many-body eigenenergies of the isolated dot at strong interaction, confirming that the dot becomes effectively decoupled from the leads. Furthermore, we explained the narrowing of the width of the peaks with the interaction strength, as well as the asymmetry of the peak shape, by analyzing the effective matrix elements for the dominating transitions.

The current tendency towards the development of smaller MOSFETs [10,11] is likely to lead to regimes where the theoretical concepts discussed in this work could be properly applied. It would be interesting to further develop our model in order to bridge the gap with those experiments. Addressing the effects of finite temperature, longer range interactions, and electron spin are envisioned, as well as going beyond the one-dimensional case. The newly developed method of obtaining non-linear conductances from time-dependent DMRG [14] could be applied to our model, and it would be interesting to study the suppression of Coulomb blockade by the bias voltage.

We acknowledge useful discussions with M. Hofheinz, G.-L. Ingold, R. A. Molina, J.-L. Pichard and M. Sanquer. We thank P. Schmitteckert for discussions and for providing his DMRG code.

References

1. L. P. Kouwenhoven, C. M. Marcus, P. L. McEuen, S. Tarucha, R. M. Westervelt, and N. S. Wingreen, in *Mesoscopic electron transport*, edited by L. L. Sohn, L. P. Kouwenhoven, and G. Schön (1997).
2. C. W. J. Beenakker, *Phys. Rev. B* **44**, 1646 (1991).
3. B. W. Alphenaar, A. A. M. Staring, H. van Houten, M. A. A. Mabesoone, O. J. A. Buyk, and C. T. Foxon, *Phys. Rev. B* **46**, 7236 (1992).
4. I. K. Marmorosk and C. W. J. Beenakker, *Phys. Rev. B* **46**, 15562 (1992).
5. I. L. Aleiner, P. W. Brouwer, and L. I. Glazman, *Phys. Rep.* **358**, 309 (2002).
6. P. W. Brouwer, A. Lamacraft, and K. Flensberg, *Phys. Rev. B* **72**, 075316 (2005).
7. Y. V. Nazarov, *Phys. Rev. Lett.* **82**, 1245 (1999).
8. D. S. Golubev and A. D. Zaikin, *Phys. Rev. B* **69**, 075318 (2004).
9. A. G. Huibers, S. R. Patel, C. M. Marcus, P. W. Brouwer, C. I. Duruöz, and J. S. Harris, Jr., *Phys. Rev. Lett.* **81**, 1917 (1998).
10. M. Boehm, M. Hofheinz, X. Jehl, M. Sanquer, M. Vinet, B. Prevtali, B. Fraboulet, D. Mariolle, and S. Deleonibus, *Phys. Rev. B* **71**, 033305 (2005).
11. M. Hofheinz, X. Jehl, M. Sanquer, G. Molas, M. Vinet and S. Deleonibus, arXiv:cond-mat/0504325.
12. Y. Nisikawa and A. Oguri, arXiv:cond-mat/0511182.
13. D. Bohr, P. Schmitteckert, and P. Wölfle, *Europhys. Lett.* **73**, 246 (2006).
14. G. Schneider and P. Schmitteckert, arXiv:cond-mat/0601389.

15. Y. M. Blanter, A. D. Mirlin, and B. A. Muzykantskii, *Phys. Rev. Lett.* **78**, 2450 (1997).
16. A. Cohen, K. Richter, and R. Berkovits, *Phys. Rev. B* **60**, 2536 (1999).
17. R. A. Molina, D. Weinmann, R. A. Jalabert, G.-L. Ingold, and J.-L. Pichard, *Phys. Rev. B* **67**, 235306 (2003).
18. R. A. Molina, P. Schmitteckert, D. Weinmann, R. A. Jalabert, G.-L. Ingold, and J.-L. Pichard, *Eur. Phys. J. B* **39**, 107 (2004).
19. G. Vasseur, D. Weinmann and R. A. Jalabert, unpublished.
20. R. A. Molina, D. Weinmann, and J.-L. Pichard, *Eur. Phys. J. B* **48**, 243 (2005).
21. T. Rejec and A. Ramšak, *Phys. Rev. B* **68**, 035342 (2003).
22. J. Favand and F. Mila, *Eur. Phys. J. B* **2**, 293 (1998).
23. O. P. Sushkov, *Phys. Rev. B* **64**, 155319 (2001).
24. V. Meden and U. Schollwöck, *Phys. Rev. B* **67**, 193303 (2003).
25. *Density-Matrix Renormalization – A New Numerical Method in Physics*, ed. by I. Peschel, X. Wang, M. Kaulke and K. Hallberg, Springer (Berlin/Heidelberg, 1999).
26. P. Schmitteckert, Ph.D. thesis (Univ. Augsburg, 1996).
27. J. Friedel, *Phil. Mag.* **43**, 153 (1952).
28. J. S. Langer and V. Ambegaokar, *Phys. Rev.* **121**, 1090 (1961); D. C. Langreth, *Phys. Rev.* **150**, 516 (1966).
29. R. A. Molina, D. Weinmann, and J.-L. Pichard, *Europhys. Lett.* **67**, 96 (2004).
30. A. Oguri, *Phys. Rev. B* **59**, 12240 (1999).
31. R. H. M. Smit, C. Untiedt, G. Rubio-Bollinger, R. C. Segers, and J. M. van Ruitenbeek, *Phys. Rev. Lett.* **91**, 076805 (2003).
32. F. Selva and D. Weinmann, *Eur. Phys. J. B* **18**, 137 (2000).
33. A. Oguri and A. C. Hewson, *J. Phys. Soc. Jpn.* **74**, 988 (2005).
34. G. Vasseur, Ph.D. thesis, in preparation (ULP Strasbourg, 2006).